

Modeling of Functionally Graded Material Shells

Sihame Khalil^{*}, *Oussama Elmhaia*⁴, *Abdellah Hamdaoui*¹, *Bouazza Braikat*¹, *Heng Hu*³,
*Adnane Boukamel*², and *Noureddine Damil*^{1,2}

¹Hassan II University of Casablanca, Laboratoire d'Ingénierie et Matériaux LIMAT, B.P 7955 Sidi Othman, Casablanca, Morocco

²Central Casablanca, Centre de Recherche Systèmes Complexes et interactions, Ville Verte, Bouskoura, 27182, Morocco

³Ningxia University, School of Mathematics and Statistics, Yinchuan 750021, China

⁴Hassan First University of Settat, Ecole Nationale des Sciences Appliquées, LAMSAD Laboratory, Berrechid 26100, Morocco

Abstract. In this research, we propose an algorithm to study the buckling of thin Functionally Graded Material (FGM) shells, utilizing a novel implementation of the asymptotic numerical method (ANM). Our approach integrates a three-step process: representation of variables and loading conditions through a truncated Taylor series, discretization using the finite element method (FEM), and advancement via a continuation method. This method is particularly effective for tracking the solution curve through systematic matrix inversion and tolerance adjustments. By applying this robust algorithm within the framework of Kirchhoff-Love theory, we analyze how the properties of FGM shells vary smoothly from metal at the base to ceramic at the surface, crucial for applications in aeronautics and civil engineering where stability under load is paramount. The results are validated against the Abaqus industrial code, demonstrating the accuracy of our model. Furthermore, we detail the impact of the volume fraction index on the load-displacement behavior and structural deformations, providing valuable insights for enhancing the design and safety of these critical structures.

1 Introduction

The advent of modern technologies necessitates the utilization of composite materials characterized by high mechanical properties tailored to specific applications yet maintaining low density. Due to their low density, combined with high strength and rigidity, composite structures have become indispensable in aerospace and aeronautics. Among these, Functionally Graded Materials (FGMs) stand out for their unique capacity to vary properties as per specific requirements. This study focuses on the behavior of FGM shells, as illustrated in figure 1.

* Corresponding author: khalile.siham@gmail.com

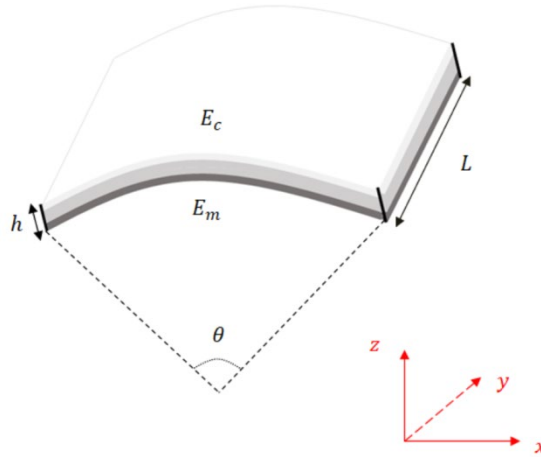


Fig. 1. Geometry of an FGM Shell.

Recent literature has extensively explored the behavior of FGM structures. For instance, the authors in [1] provided analytical solutions for the bending, vibration, and buckling of FGM plates, while the research in [2] investigated the vibration and stability of conical shells made from functional gradient materials. A static analysis of an aircraft wing composed of FGMs using a multi-layer finite element model was detailed in [3]. The study in [4] explored the effects of notches and coatings on peak stresses in cylindrical contacts within FGMs, and Mobtasem et al. [5] applied FGM techniques to reduce the impact of holes in fiber-reinforced polymers.

In our work, we conduct a numerical analysis of the buckling behavior of FGM shells, which vary in property distribution along their thickness, employing a shell model based on Kirchhoff-Love theory. Understanding the buckling of thin shells is crucial for preventing sudden failures, enhancing design efficiency, and improving structural safety. This enables the development of lighter and stronger shells, facilitating a deeper understanding of their response under various load conditions and identifying methods to fortify them.

Our analysis utilizes the numerical asymptotic method (ANM), which represents the problem's unknowns and loading parameters as a truncated Taylor series, with each term addressing a linear problem. This approach is essential for employing the continuation method, crucial when navigating near bifurcation points. The continuation method systematically advances along the solution curve, adjusting the step size based on the convergence radius of the series, thus ensuring the path follows accurately even near critical transitions. The finite element method discretizes these problems using planar elements, which are adapted to the shell's curved surfaces through a passage matrix. Subsequently, the accuracy and reliability of our results are validated by benchmarking against those obtained from the industrial standard Abaqus code.

2 Modeling of FGM Shells

In this work, the theory of thin shells assumes that the shell thickness is considerably less than its radius of curvature, minimizing shear effects. Consequently, the results from this theory align closely with those from broader theories like Mindlin's, except when dealing

with thicker shells where Mindlin's theory provides more accurate outcomes due to its consideration of higher-order deformations. Thin-shell theory fundamentally relies on mathematical equations that articulate the material behavior. Boundary conditions play a crucial role in this context, defining the interactions between the model and its environment by specifying stresses or displacements at the shell edges. This setup allows the system's behavior to be described uniquely. The components of the displacement vector for a point at a distance z from the mid-surface of the shell are defined in a way that captures the essential mechanical characteristics and can be expressed as follows [6,7]:

$$\begin{cases} U(x, y, z) = u(x, y) + z\beta_x(x, y) \\ V(x, y, z) = v(x, y) + z\beta_y(x, y) \\ W(x, y, z) = w(x, y) \end{cases} \quad (1)$$

where $u(x, y)$, $v(x, y)$ and $w(x, y)$ correspond to the displacements of the point located on the mid-surface of the shell, and where $\beta_x(x, y)$ and $\beta_y(x, y)$ are respectively the rotations about the axes o_x and o_y .

2.1 Strain vector and stress vector

In Kirchhoff–Love's theory, the deformation vector is given by:

$$\{\gamma\} = \{e\} + z\{k\} \quad (2)$$

The membrane deformations $\{e\}$ and the curvature $\{k\}$ of the mean plane of the ω_0 structure are given by:

$$\{e\} = \begin{Bmatrix} e_{xx} \\ e_{yy} \\ 2e_{xy} \end{Bmatrix} = \begin{Bmatrix} u_{,x} + \frac{1}{2}w_{,x}^2 \\ v_{,y} + \frac{1}{2}w_{,y}^2 \\ u_{,y} + v_{,x} + w_{,x}w_{,y} \end{Bmatrix}, \quad \{k\} = \begin{Bmatrix} k_{xx} \\ k_{yy} \\ 2k_{xy} \end{Bmatrix} = \begin{Bmatrix} \beta_{x,x} \\ \beta_{y,y} \\ \beta_{x,y} + \beta_{y,x} \end{Bmatrix} \quad (3)$$

The stress vector in the case of plane stresses for the FGM shell model, whose material properties vary continuously through the thickness of the shell, is expressed by the following constitutive law [8]:

$$\begin{Bmatrix} S_{11} \\ S_{22} \\ S_{12} \end{Bmatrix} = \frac{E(z)}{1-\nu^2} \begin{bmatrix} 1 & \nu & 0 \\ \nu & 1 & 0 \\ 0 & 0 & \frac{1-\nu}{2} \end{bmatrix} \begin{Bmatrix} \gamma_{11} \\ \gamma_{22} \\ 2\gamma_{12} \end{Bmatrix} \quad (4)$$

where ν denotes the Poisson coefficient. The variation of Young's modulus as a function of thickness is given by the following mixing law:

$$E(z) = (E_c - E_m)V_c(z) + E_m \quad (5)$$

where E_c and E_m are, respectively, the Young's moduli of the upper and lower surfaces of the FGM shell, and V_c is the volume fraction expressed according to a power law :

$$V_c(z) = (1/2 + z/h)^k \quad (6)$$

The parameter k represents the volume fraction index determining the percentage of ceramic and metal in the mixture.

The principle of virtual work and the constitutive law can be written in the following form:

$$\begin{cases} \int_{\omega} \langle \delta \Gamma \rangle \{S\} d\omega = \lambda \int_{\partial\omega} \langle \delta \mathbf{U} \rangle \{F\} dl \\ \{S\} = [D]\{\Gamma\} \end{cases} \quad (7)$$

where λF are the applied external forces proportional to a load parameter λ , $\langle \mathbf{U} \rangle = \langle u, v, w \rangle$ is the generalized displacement and $\{S\}$ and $\{\Gamma\}$ are the generalized stress vector and strain vector [9].

We denote by $[D]$ the generalized behavior matrix:

$$[D] = \begin{bmatrix} C_1 & C_1\nu & 0 & C_2 & C_2\nu & 0 \\ C_1\nu & C_1 & 0 & C_2\nu & C_2 & 0 \\ 0 & 0 & \frac{C_1(1-\nu)}{2} & 0 & 0 & \frac{C_2(1-\nu)}{2} \\ C_2 & C_2\nu & 0 & C_3 & C_3\nu & 0 \\ C_2\nu & C_2 & 0 & C_3\nu & C_3 & 0 \\ 0 & 0 & \frac{C_2(1-\nu)}{2} & 0 & 0 & \frac{C_3(1-\nu)}{2} \end{bmatrix} \quad (8)$$

where $C_1 = \int_{-\frac{h}{2}}^{\frac{h}{2}} E(z) dz$, $C_2 = \int_{-\frac{h}{2}}^{\frac{h}{2}} z E(z) dz$ and $C_3 = \int_{-\frac{h}{2}}^{\frac{h}{2}} z^2 E(z) dz$.

We numerically solve the nonlinear equations (7) using the ANM algorithm [8]. The principle of ANM is to search the unknowns of the initial non-linear problem and the loading parameter in the form of a Taylor series representation truncated at an order N . The terms of these Taylor series are then solutions of linear problems. By discretizing these linear problems using the Finite Element Method, a large part of the solution branch is obtained by inverting a single stiffness matrix. Iteration of this procedure then yields the entire solution curve by continuation and specification of a tolerance parameter.

3 Results and Discussions

Consider an elastic FGM cylindrical shell with a length of $L = 254\text{mm}$, a radius of $R = 2540\text{mm}$, a half-opening angle of $\theta = 0.1\text{rad}$, and a thickness of $h = 6.35\text{mm}$ or $h = 12.7\text{mm}$, with Young's moduli $E_c = 380\text{GPa}$, $E_m = 70\text{GPa}$, and a Poisson's ratio $\nu = 0.3$. The shell is subjected to a point load λF with $F = 1000\text{N}$. The openings are free, and the other two edges are simply supported with $u = 0$, $w = 0$, and $\theta_x = 0$ (see figure 2). The results of this test will be compared to those obtained using Abaqus with the Riks method and the *STR13* element.

For symmetry reasons, a quarter of the cylindrical shell is discretized with 11 nodes along the length and 11 nodes following the shell opening. The parameters for the ANM are: $N = 20$ for the truncation order and $\varepsilon = 10^{-6}$ for the tolerance parameter.

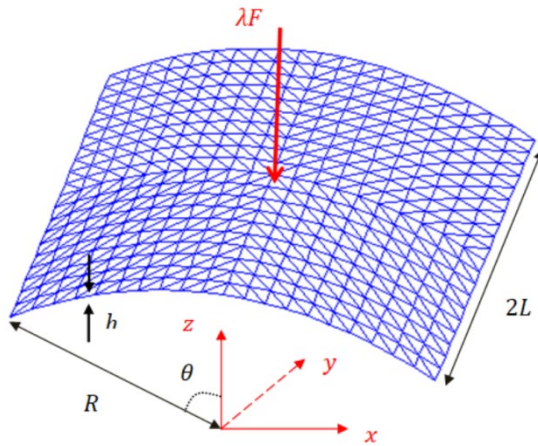


Fig. 2. Geometric characteristics of an elastic cylindrical shell made of functionally graded material (FGM).

In our model, where the thickness is considered small compared to the radius of curvature and shear effects are negligible, the results of this work remain similar to those obtained with other theories dealing with thin shells, as we use small thicknesses.

Figures 3 and 4 show the load-displacement curve at the shell's central node and its deformation. For the FGM shell of thickness $h = 6.35\text{mm}$ and $h = 12.7\text{mm}$.

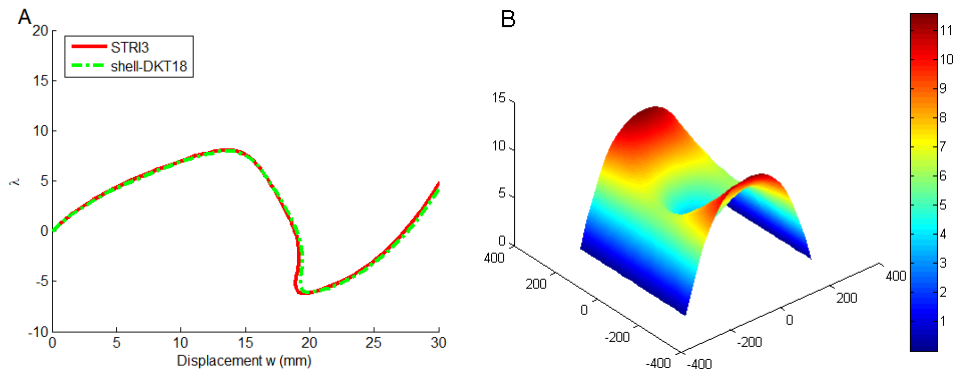


Fig. 3. Buckling of a cylindrical shell for $h = 6.35\text{mm}$ and $k = 2$: (A) Load-displacement curve at the center node obtained by the 'shell-DKT18' model and by Abaqus, (B) Deformation of the structure studied at $(\lambda = 7)$.

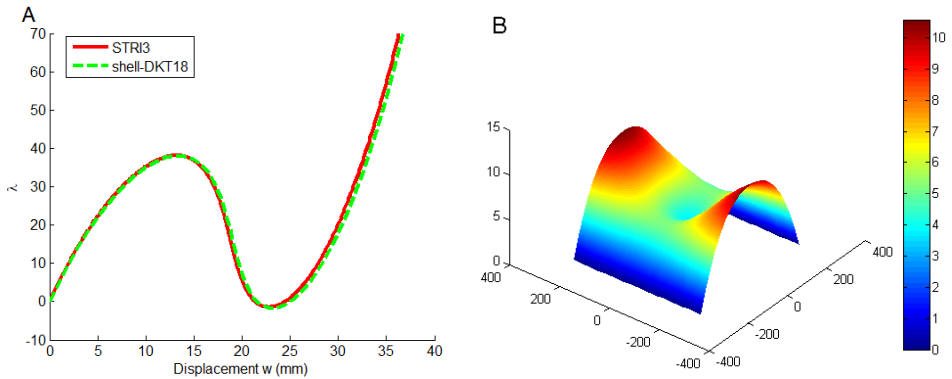


Fig. 4. Buckling of a cylindrical shell for $h = 12.7\text{mm}$ and $k = 2$: (A) Load-displacement curve at the center node obtained by the 'shell-DKT18' model and by Abaqus, (B) Deformation of the structure studied at ($\lambda = 33.05$).

From figures 3 and 4, we can see that our 'shell-DKT18' model faithfully reproduces the curves presented by the Abaqus industrial code. We can also observe that the load-displacement curve shows buckling at two limit points.

Figure 5 shows the effect of the volume fraction index k on the load-displacement curve at the central node of the FGM shell of thicknesses $h = 6.35\text{mm}$ and $h = 12.7\text{mm}$.

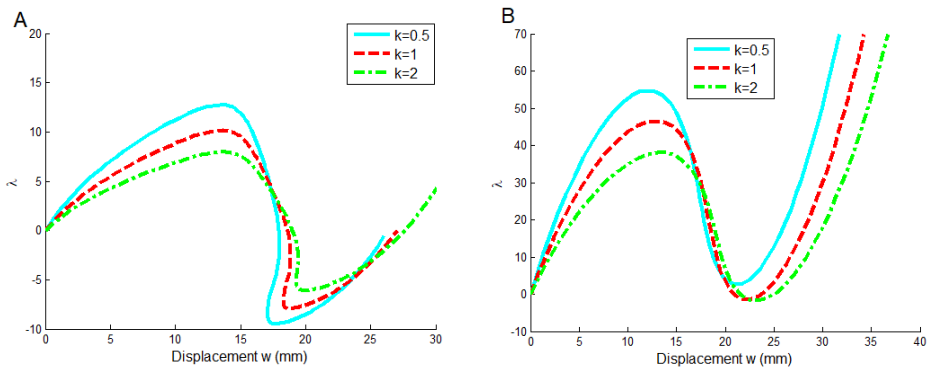


Fig. 5. Impact of k on the load-displacement curve at the center of the FGM shell obtained with the 'shell-DKT18' model: (A) for $h = 6.35\text{mm}$, (B) for $h = 12.7\text{mm}$.

From figure 5, we can see that the $h = 12.7\text{mm}$ shell shows high resistance to buckling with a higher critical load of the first limit point compared to the $h = 6.35\text{mm}$ shell.

In Table 1, the coordinates of the maximum point ($Coor_{Max}$) and the coordinates of the minimum point ($Coor_{Min}$) are presented for different values of the volume fraction index k , for thicknesses $h = 6.35\text{mm}$ and $h = 12.7\text{mm}$.

Table 1. Impact of k on the values of the coordinates of the maximum point ($Coor_{Max}$) and the minimum point ($Coor_{Min}$): (A) for ($h = 6.35mm$), (B) for ($h = 12.7mm$).

	k=0.5				k=1				k=2			
	(A)		(B)		(A)		(B)		(A)		(B)	
	x	y	x	y	x	y	x	y	x	y	x	y
$Coor_{Max}$	14	12.7	12	55	13.6	10	12.7	46.6	13.4	8	13	38
$Coor_{Min}$	17.7	-9.4	21.2	2.7	18.8	-8	22	-1.3	19.8	-6.1	23	-1.7

Table 1 demonstrates the effect of varying the volume fraction index k on the coordinates of maximum $Coor_{Max}$ and minimum $Coor_{Min}$ points across FGM shells with two different thicknesses. As k increases, the vertical position (y-coordinate) of $Coor_{Max}$ consistently decreases for both shell thicknesses, indicating a lowering of the peak stress or deformation point. Conversely, the response of $Coor_{Min}$'s vertical position to changes in k differs based on shell thickness, highlighting how material gradation affects structural behavior under load.

3 Conclusion

This study numerically explores the behavior of Functionally Graded Material (FGM) shells with two distinct thicknesses: $h = 6.35mm$ and $h = 12.7mm$, while adjusting the volume fraction index k . The findings indicate that the shell with a thickness of $h = 12.7mm$ exhibited enhanced buckling strength and was able to withstand higher critical loads. Furthermore, the volume fraction index was found to significantly influence the critical load. These insights pave the way for further research, particularly in developing and applying theories suitable for analyzing thicker materials, such as the Reissner-Mindlin theory.

Acknowledgment

This work has been supported by the National Key R&D Program of China (Grant No. 2022YFE0113100).

References

1. J. Kim, J.N. Reddy, Analytical solutions for bending, vibration, and buckling of FGM plates using a couple stress-based third-order theory, *Compos. Struct*, **103**, 86-98 (2013)
2. A.H. Sofiyev, The vibration and stability behavior of freely supported FGM conical shells subjected to external pressure, *Compos. Struct*, **89**, 356-366 (2009)
3. DH. Kim, M. Amir, SW. Kim, Static analysis of shear-deformable aircraft wings using a multilayered functionally graded material model, *Adv. Compos. Mater*, **33**, 479-503 (2024)
4. P. Pradhan, H. Murthy, Application of undercut and FGM to mitigate stress gradients in cylindrical contacts, *J. Strain Anal*, 03093247241273818 (2024)

5. M. Mobtasem, AA. Abd-Elhady, HEM. Sallam, Implementation of a new approach based on the functionally graded materials concept to improve the strength of laminated composites containing open-hole, *Polym. Compos*, **45**, 12132-12146 (2024)
6. S. Khalil, y. Belaasilia, A. Hamdaoui, B. Braikat, N. Damil, M. Potier-Ferry, A reduced-order modeling based on multi-scale method for wrinkles with variable orientations, *Int. J. Solids Struct*, **207**, 89-103 (2020)
7. S. Khalil, y. Belaasilia, A. Hamdaoui, B. Braikat, M. Jamal, N. Damil, Z. Azari, ANM analysis of a wrinkled elastic thin membrane, *C. R.. Mec*, **347**, 701-709 (2019)
8. S. Khalil, O. Elmhaia, A. Hamdaoui, B. Braikat, H. Hu, A. Boukamel, N. Damil, Analysis of wrinkling in FGM membrane using the asymptotic numerical method. in: Proceedings of the 4th International Conference on Innovative Research in Applied Science, Engineering and Technology (IRASET), IEEE, 1–5, May 2024, Fès, Maroc (2024)
9. S. Khalil, O. Elmhaia, B. Braikat, A. Hamdaoui, H. Hu, A. Boukamel, N. Damil, Investigation of fgm membrane wrinkling using reduced models based on a multi-scale method, *Thin.Walled Struct*, **199**, 111834 (2024)
10. B. Cochelin, N. Damil, M. Potier-Ferry, Méthode asymptotique numérique, (Hermès Lavoisier, paris, 298(2007)